ELSEVIER

Chemical Geology 195 (2003) 159–179

CHEMICAL GEOLOGY
INCLUDING
ISOTOPE GEOSCIENCE

www.elsevier.com/locate/chemgeo

Reduced sulfur in euxinic sediments of the Cariaco Basin: sulfur isotope constraints on organic sulfur formation

Josef P. Werne[a,b,*], Timothy W. Lyons[c], David J. Hollander[a,1], Michael J. Formolo[c], Jaap S. Sinninghe Damsté[b]

[a] *Department of Geological Sciences, Northwestern University, Evanston, IL 60208, USA*
[b] *Department of Marine Biogeochemistry and Toxicology, Netherlands Institute for Sea Research (NIOZ), P.O. Box 59, 1790 AB Den Burg, Texel, The Netherlands*
[c] *Department of Geological Sciences, University of Missouri, Columbia, MO 65211, USA*

Received 28 March 2001; received in revised form 15 November 2001

Abstract

Reduced sulfur accumulation in Holocene and latest Pleistocene euxinic marine sediments from the Cariaco Basin, Venezuela, was investigated to constrain the timing and possible pathways of organic matter (OM) sulfurization. Data were collected for a diverse suite of sulfur species, including concentrations and sulfur isotope compositions of pore-water sulfide, pore-water sulfate, pyrite sulfur, total organic sulfur (TOS), kerogen sulfur (KS), and polar bitumen sulfur (PBS). Results suggest that there was a period during which almost no diagenetic pyrite formed in the sediments of the Cariaco, coincident with a shift from high to lower sedimentation rates and a concomitant change in the delivery of organic matter to the sediments. The sulfur isotope composition of organic matter was predicted based on assumed pathways using weighted isotopic mass balance calculations and compared to measured isotope values for organic sulfur. These results indicate that organic sulfur is derived primarily from pore-water sulfide, with minor contributions from primary bio-sulfur (e.g., in proteins derived from algae and bacteria). The predicted sulfur isotope values of organic sulfur compounds (OSC) suggest that pore-water sulfide is the ultimate source of reduced sulfur for incorporation into organic matter. It is possible, however, that reactive sulfur intermediates such as elemental sulfur or polysulfides react directly with organic matter. These intermediate sulfur species are likely formed through partial oxidation of sulfide by anaerobic sulfide-oxidizing microbes living in the sediments.

Keywords: Organic sulfur; Inorganic sulfur; Sulfur isotopes; Sedimentary sulfur cycling; Cariaco basin

1. Introduction

The sequestration of various forms of reduced sulfur in sediments has been shown to affect the biogeochemical cycles of sulfur, carbon, and oxygen, thereby affecting the evolution of atmospheric CO_2 and O_2 concentrations over geologic time (Holland, 1973; Garrels and Lerman, 1981; Berner, 1987;

* Corresponding author. Current address: Large Lakes Observatory and Department of Chemistry, University of Minnesota Duluth, Duluth, MN 55812, USA. Tel.: +1-218-726-7435; fax: +1-218-726-6979.
E-mail address: jwerne@d.umn.edu (J.P. Werne).
[1] Current address: Department of Marine Science, University of South Florida, St. Petersburg, FL 33701, USA.

0009-2541/02/$ - see front matter © 2002 Elsevier Science B.V. All rights reserved.
doi:10.1016/S0009-2541(02)00393-5

Petsch and Berner, 1998; Canfield et al., 2000). The formation of pyrite is generally assumed to be the most quantitatively significant sink for reduced sulfur in the marine environment (Garrels and Lerman, 1984; Berner and Raiswell, 1983; Kump and Garrels, 1986). A second significant, and often neglected, sink for sulfur during early diagenesis is the incorporation of reduced sulfur into organic matter (OM) (Zaback and Pratt, 1992; Anderson and Pratt, 1995; Canfield et al., 1998a). Organic matter sulfurization has also been identified as an important mechanism for the preservation of functionalized organic compounds during early diagenesis (Sinninghe Damsté and de Leeuw, 1990; Kohnen et al., 1991a). Despite such significance, the timing and specific reaction pathway(s) of pyrite and organic sulfur formation are still subjects of study and debate.

In order for either pyrite formation or OM sulfurization reactions to occur, certain conditions of the sedimentary environment must be met. First, an adequate supply of inorganic sulfide (i.e., H_2S) must be present, which implies anoxic conditions and the occurrence of microbial sulfate reduction. The supply of dissolved sulfide is controlled by the rate of bacterial sulfate reduction according to the generalized reaction:

$$2CH_2O + SO_4^{2-} \rightarrow H_2S + 2HCO_3^-$$

(Berner, 1984) and the initial supply and rate of replenishment of SO_4. The resulting dissolved sulfide is then utilized in the formation of both pyrite and organic sulfur.

Whether the sulfide provided by bacterial sulfate reduction is then consumed during the formation of iron sulfide or by the sulfurization of OM is dependent on the availability of reactive iron species (e.g., iron oxides and oxyhydroxides, Canfield, 1989; Canfield et al., 1992, 1996). If reactive iron is readily available, pyrite formation is believed to be a kinetically favored process compared to sulfurization of OM (Gransch and Posthuma, 1974; Hartgers et al., 1997).

Finally, there must be sufficient initial inputs of reactive OM to stimulate sulfate reduction and react with sulfur as well as a minimum of secondary reworking of sediments by burrowing heterotrophs so the sediments can remain anoxic. Anoxic and euxinic conditions are critical for the enrichment of reduced sulfur in sedimentary environments, in part for the enhanced deposition of reduced sulfur, but also for the significantly enhanced preservation of reduced forms through the elimination of bioturbation and concomitant oxidation. Additional controls on pyrite formation and OM sulfurization include sedimentation rates, sedimentary and water column redox conditions, and the sulfur species available (e.g., Berner 1970, 1984; Lyons and Berner, 1992; Calvert et al., 1996; Wilkin et al., 1997; Raiswell and Canfield, 1998).

Among the remaining questions is the extent to which reactive intermediates [e.g., elemental sulfur (S°) or polysulfides (S_x^-)] play a role in organic sulfur or pyrite formation relative to direct reaction with H_2S (cf., Berner, 1970; Rickard, 1975; Boesen and Postma, 1988; Sinninghe Damsté et al., 1989a; Kohnen et al., 1991b; Middelburg, 1991; Schoonen and Barnes, 1991a,b). Numerous laboratory (e.g., Schouten et al., 1994; Wilkin and Barnes, 1996; Rickard and Luther, 1997; Kok et al., 2000a) and field studies (e.g., Goldhaber and Kaplan, 1974; Raiswell and Berner, 1985; Sinninghe Damsté et al., 1988; Kohnen et al., 1990; Middelburg, 1991; Canfield et al., 1992, 1998a; Putschew et al., 1995, 1996; Hurtgen et al., 1999; Werne et al., 2000a) have attempted to constrain the reactions involved in pyrite and organic sulfur formation. In actuality, multiple reaction pathways for both pyrite formation and OM sulfurization may be occurring. For example, various studies have called upon a number of specific mechanisms of organic matter sulfurization, including photochemical reactions (Adam et al., 1998), reactions with polysulfides (Aizenshtat et al., 1983; Schouten et al., 1994), and reaction with H_2S (Werne et al., 2000a).

There is a significant sulfur isotope fractionation associated with the bacterially mediated conversion of sulfate to sulfide, typically ranging from approximately 20‰ to 45‰ (Hartmann and Nielsen, 1969; Goldhaber and Kaplan, 1974; Chambers and Trudinger, 1979; Habicht and Canfield, 1997; Brüchert et al., 2001) though fractionations as small as 2‰ (Detmers et al., 2001) and as large as 72‰ (Wortmann et al., 2001) have been observed. It is generally believed that any sulfur isotope fractionation associated with the formation of pyrite from

sulfide or sulfur intermediates is negligible (~ 1‰, Price and Shieh, 1979; Wilkin and Barnes, 1996; Böttcher et al., 1998a), particularly when compared to the magnitude of the isotope discrimination associated with sulfate reduction (biological or chemical). The same is expected for organic sulfur compounds (OSC). Therefore, the sulfur isotope composition of sedimentary organic sulfur should indicate the source, and thus timing and reaction pathways of sulfur incorporation into OM.

Sediments from the Cariaco Basin, Venezuela, provide an ideal location to study reduced sulfur deposition in marine sediments in general, and early diagenetic sulfurization of OM in particular. High primary productivity in the surface waters provides a large supply of functionalized OM that is available for sulfurization, some of which persists to depths of more than 6 m below the sediment–water interface, suggesting sufficient OM concentrations for reactions with sulfur (Werne et al., 2000a,b). The sediments and bottom waters below ~ 300 m have been anoxic, and possibly euxinic, for the past 12.6 ^{14}C ky/14.5–15 calendar ky (Richards, 1975; Peterson et al., 1991; Hughen et al., 1996a,b, 1998; Lin et al., 1997) thereby preventing reworking by burrowing heterotrophs. Currently, there is free sulfide in the water column below ~ 300 m (Wakeham, 1990; Fry et al., 1991), suggesting that microbial sulfate reduction is an active process in the Cariaco Basin sediments and likely the water column. The iron sulfide system is ultimately limited by the availability of readily reactive iron (Lyons et al., 2003, this volume), making the sulfurization of OM a likely process.

The present study is an analysis of the processes of pyrite formation and OM sulfurization as they occur in the sediments of the Cariaco Basin, Venezuela. The analytical focus is on the major species of sulfur, including pore-water sulfate and sulfide, pyrite sulfur, and the major forms of organic sulfur (dominantly kerogen sulfur) (see also Lyons et al., 2003, this volume). An interval with excellent temporal control through correlation to a well-dated adjacent core (Lin et al., 1997) was used for analyses of both concentrations and isotope compositions of the various species of organic and inorganic sulfur. Comparison of the inorganic and organic sulfur data shows that pyrite and organic sulfur formation are competing processes and provides insights into the timing and possible pathways of both pyrite and organic sulfur formation in marine sediments. Sulfur isotope data indicate that pyrite in the Cariaco Basin is formed both in the water column (syngenetically) and in the sediments (diagenetically) and that pyrite accumulation has varied significantly over the past 12 ^{14}C ky. Additional sulfur isotope constraints suggest that organic sulfur is derived primarily from pore-water sulfide, though whether the sulfide reacts directly with organic matter or is incorporated indirectly via reactive intermediates such as polysulfides remains unresolved. Furthermore, the sulfur isotope data suggest the existence of an active anaerobic sulfide oxidizing microbial community in Cariaco Basin sediments.

2. Methods

2.1. Site description, sampling, and age control

The Cariaco Basin is a pull-apart basin located on the continental shelf immediately north of Venezuela (Fig. 1). It consists of two sub-basins, with a maximum depth of about 1400 m, separated by a saddle at 900 m. Samples were collected from ODP Site 165 (Core 1002B) on the western side of the saddle at about 900 m water depth (Shipboard Scientific Party, 1997). Sediments were frozen immediately after collection, stored frozen for several months, and dried in an oven at 50 °C. Dried samples were homogenized, and splits were taken for the various analyses. Sampling resolution ranged from 5 to ~ 100 cm, depending on the labor intensity of the given analytical procedure (i.e., pore-water and sedimentary inorganic sulfur and bulk organic sulfur measurements were made at higher resolution than the measurements of extracted organic sulfur). Age control for this study was provided by a suite of accelerator mass spectrometer (AMS) ^{14}C dates on individual planktonic foraminifera from core PL07-39PC (Lin et al., 1997), which were correlated to 1002B using magnetic susceptibility (Shipboard Scientific Party, 1997; Werne et al., 2000b). The study interval spans the last ~ 12 ^{14}C ky (14.5–15 calendar ky; Peterson et al., 1991; Hughen et al., 1996a,b, 1998; Lin et al., 1997).

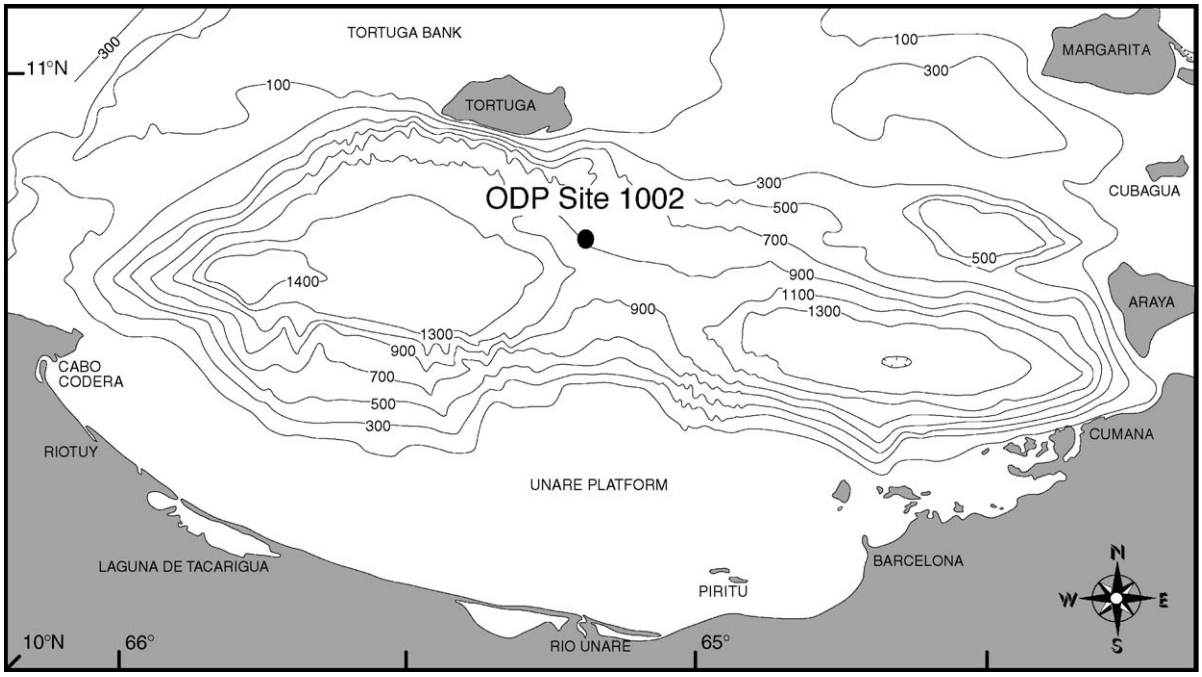

Fig. 1. Location and bathymetry of the Cariaco Basin showing position of Site 1002, Ocean Drilling Program (ODP) Leg 165.

2.2. Pore-water sulfur

Pore-water sulfate concentrations were measured via shipboard ion chromatography. Aliquots of filtered pore-water were fixed on board in a nitrogen-filled glove bag for analysis of aqueous sulfide concentration using a 3% Zn solution and stored at 8 °C. Total dissolved sulfide concentrations were measured colorimetrically according to the methylene blue method of Cline (1969) with a detection limit of 3 μM. Aliquots of pore-water were fixed for sulfide isotope determinations using Cd acetate and stored at 8 °C. The CdS precipitates—following removal of sea water—were converted to Ag_2S via precipitation in 3% Ag nitrate with 10% NH_4OH, filtered, and dessicated in preparation for isotope measurement. Dissolved sulfate used for isotopic analysis was precipitated as $BaSO_4$, filtered, and dried in a dessicator. The precipitated $BaSO_4$ and Ag_2S samples were each homogenized with V_2O_5 catalyst, and isotope measurements were performed by combustion in a continuous flow elemental analyzer connected to a Finnigan 252 stable isotope ratio monitoring mass spectrometer (EA-irmMS) at the Indiana University Bloomington-Stable Isotopes Research Facility (IUB-SIRF). Sulfur isotope compositions are expressed as permil (‰) deviations from V-CDT using the conventional delta notation with a standard deviation of 0.1‰. Measurements were directly calibrated against multiple laboratory standards, including NBS-127 (+20.00‰ V-CDT).

2.3. Sedimentary sulfur and iron

A sequential extraction scheme (Fig. 2) was used to analyze homogenized, powdered sediments for various sulfur species. Splits of approximately 25 g were homogenized and ultrasonically extracted with methanol (MeOH) (x), MeOH/dichloromethane (DCM) 2:1, MeOH/DCM 1:1 (5 ×), MeOH/DCM 1:2 and DCM (2 ×) to obtain the total lipid extract (TLE) for analysis of bitumen sulfur. TLEs were then fractionated on an alumina column (2 × 25 cm, alumina activated for 2 h at 150 °C) by elution with 150 ml hexane/DCM (9:1 v/v) to obtain the apolar frac-

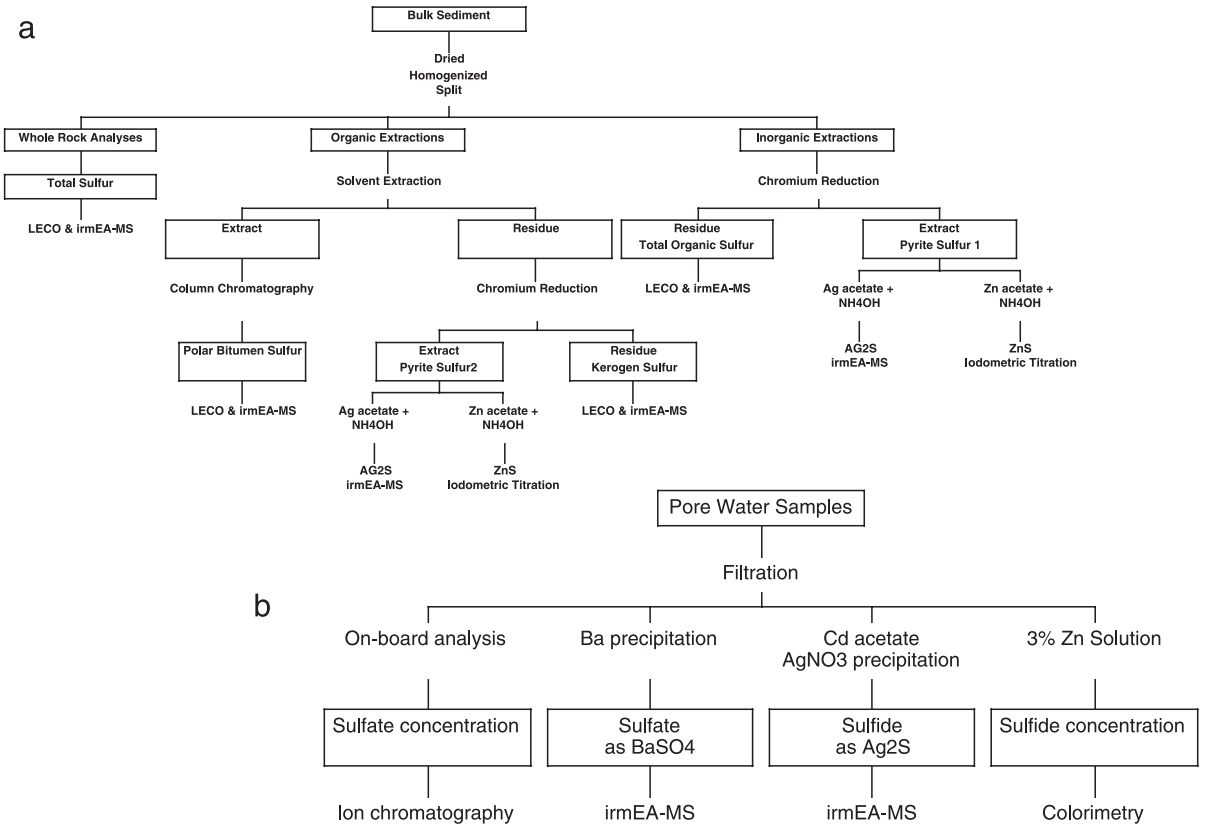

Fig. 2. Flow chart of sulfur isolation and measurement techniques. (a) Sediment samples. (b) Pore-water samples.

tion, DCM/MeOH (1:1) to obtain the polar fraction, and methanol to obtain any remaining polar OM. Polar fractions were saved for sulfur isotope analysis (polar bitumen sulfur, PBS).

Splits of the bitumen extracted sediments and bulk (whole rock) sediments were analyzed for pyrite sulfur (S_{py}) by the chromium reduction method described by Canfield et al. (1986). The H_2S evolved was driven via N_2 carrier into ~30 ml of 3% Zn acetate with 10% NH_4OH and trapped as ZnS for quantification by iodimetric titration. Additional aliquots were trapped as Ag_2S for isotope measurement using ~30 ml 3% Ag nitrate with 10% NH_4OH (Newton et al., 1995). The Cr-reduction method is generally specific to reduced inorganic forms of sulfur (Canfield et al., 1986). Representative analyses indicated insignificant amounts of acid volatile sulfides (AVS, see Lyons et al., 2003, this volume), and concentrations of elemental sulfur are expected to be low relative to iron sulfide in these reducing sediments. Thus, the Cr-reducible fraction is dominantly pyrite. Differences between the two pyrite determinations (bitumen extracted and whole rock) were insignificant, confirming that the chromium reduction method does not extract organic sulfur.

The residues after chromium reduction were then washed (3×) with distilled, deionized water, filtered and dried in a dessicator. Splits of the filtered residues were analyzed by LECO to determine total organic sulfur (TOS, from the samples that had only undergone chromium reduction) and kerogen sulfur (KS, on the samples that had undergone bitumen extraction and chromium reduction). The various extracted sulfur species and filtered residues were then placed in either tin boats (S_{py}, TOS, KS) or silver boats (PBS) with V_2O_5 catalyst and analyzed for their sulfur isotope compositions by the continuous flow EA-irmMS method described above.

Standard deviations for these bulk measurements was better than 0.5‰ for S_{py}, TOS, and KS. The PBS sulfur isotope ratios were only measured once per sample due to small sample size, so no standard deviation is reported, however, standards interspersed with the PBS samples had precisions better than 0.5‰. It should be noted that the use of silver boats rather than tin boats for measurement of PBS sulfur isotope composition may have decreased the quality of the chromatography due to poor combustion of silver. While such an artifact was observed, the chromatography was sufficient quality to report isotopic data within an error of ±1‰. Furthermore, the interspersed standards were accurate. Thus, in the absence of extreme tailing of the PBS peak in the EA-irmMS system, the sulfur isotope measurements made on PBS are of sufficient quality for comparisons with the other pools of organic and inorganic sulfur.

Concentrations of pyrite Fe were calculated stoichiometrically assuming all S extracted by the chromium reduction method (Canfield et al., 1986) exists as FeS_2 (Lyons et al., 2003, this volume). Reactive iron has traditionally been defined as the fraction of solid-phase Fe readily solubilized in boiling 12N HCl (Berner, 1970; Raiswell et al., 1988). Recent studies, however, have shown that this may overestimate the reactive iron reservoir by solubilizing Fe silicates that are reactive only on much longer timescales (Canfield et al., 1992; Raiswell et al., 1994; Raiswell and Canfield, 1996). To account for this potential overestimation of reactive iron, we utilize data from the study of Raiswell and Canfield (1998), in which Fe in a select suite of samples from the core of the present study was extracted using buffered dithionite. This method is specific to Fe oxides and oxyhydroxides and consequently is a more accurate representation of Fe that is reactive on short timescales (e.g., Canfield, 1989; Canfield et al., 1992; Raiswell et al., 1994; Raiswell and Canfield, 1998). Reactive iron (Fe_R) for this study is therefore defined as dithionite extractable iron (Fe_D) plus pyrite iron (Fe_{py}).

2.4. Accumulations

It is well documented that during deposition of deeper Cariaco sediments (~3 to 6 m depth), the bulk sedimentation rate was much higher (~100 cm/ky compared to ~30 cm/ky during deposition of the upper sediments, Shipboard Scientific Party, 1997) due to increased inputs of terrestrial materials (e.g., Hughen et al., 1996a) and biogenic materials (OM, carbonate, and opal; Peterson et al., 1991; Hughen et al., 1996a; Werne et al., 2000b).

To normalize for possible artifacts of dilution linked to changes in bulk sedimentation rate, S_{py}, Fe_R, and KS concentrations were converted to accumulation rates ($g/cm^2/ky$). It is assumed that the accumulation rate of S_{py} represents input from pyrite formed in the water column (syngenetic pyrite) combined with pyrite formed in the sediments during progressive burial (diagenetic pyrite), and KS accumulation represents inputs of primary biogenic sulfur (e.g., in proteins) and the accumulation of diagenetically and syngenetically formed organic sulfur. Fe_R is recorded as syngenetically and diagenetically formed pyrite plus the remaining unsulfidized portion of the readily reactive detrital Fe flux (Fe_D) (Lyons et al., 2003, this volume). Therefore, these values are not true accumulation *rates* in the sense of sedimentary (detrital) deposition, but rather comprise a combination of sedimentary deposition and secondary authigenesis and will therefore be discussed as accumulations.

One potential problem with the use of accumulations for the analysis of pyrite and organic sulfur deposition in the Cariaco Basin is that a fundamental change in sedimentation rate occurs at a time when there is a plateau in the ^{14}C data (i.e., the apparent age based on ^{14}C measurements is 10 ky b.p. throughout an interval of ~1 m; Lin et al., 1997; Hughen et al., 1998). To account for this problem, the ages were interpolated between the nearest reliable data points (Lin et al., 1997), and an attempt was made to link the radiocarbon record with varves in the basin (Hughen et al. 1998). Nevertheless, this problem does increase the error involved in age estimates, thereby increasing the error in accumulation rate estimates. To compensate for this uncertainty, we have also used the ratio of organic sulfur to total organic carbon (e.g., KS/TOC) as a time independent method of normalizing the concentration data to account for sedimentary dilution effects. The input of organic matter is a fundamental control on the concentration of KS as reflected in OM available for reaction with sulfur (KS), so any increase

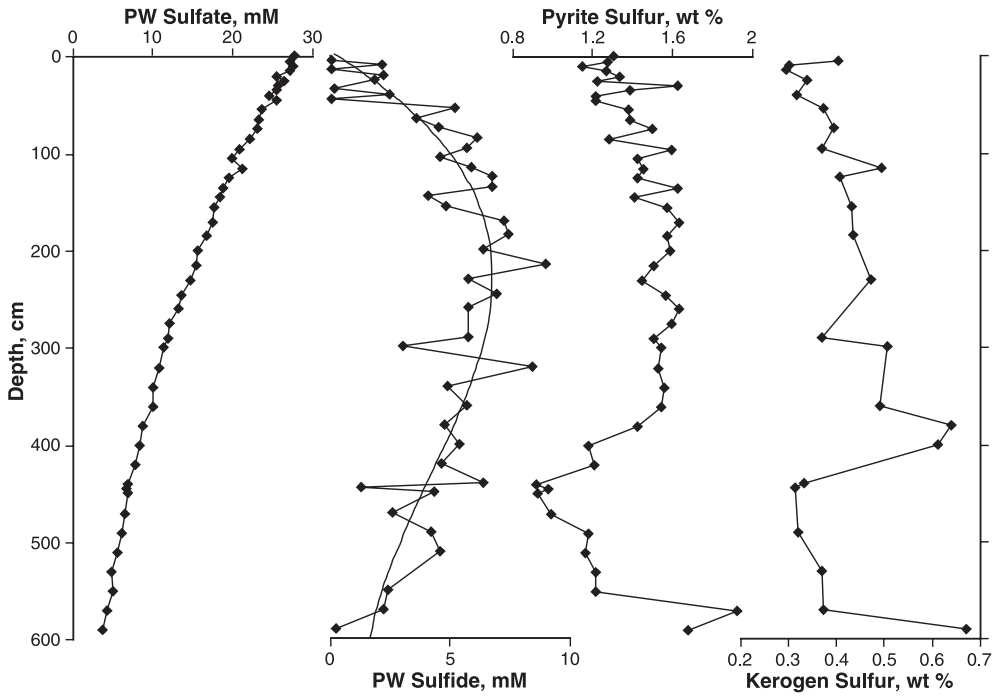

Fig. 3. Depth profiles of pore-water sulfate, pore-water sulfide, pyrite sulfur, and kerogen sulfur concentration in sediments of the Cariaco Basin.

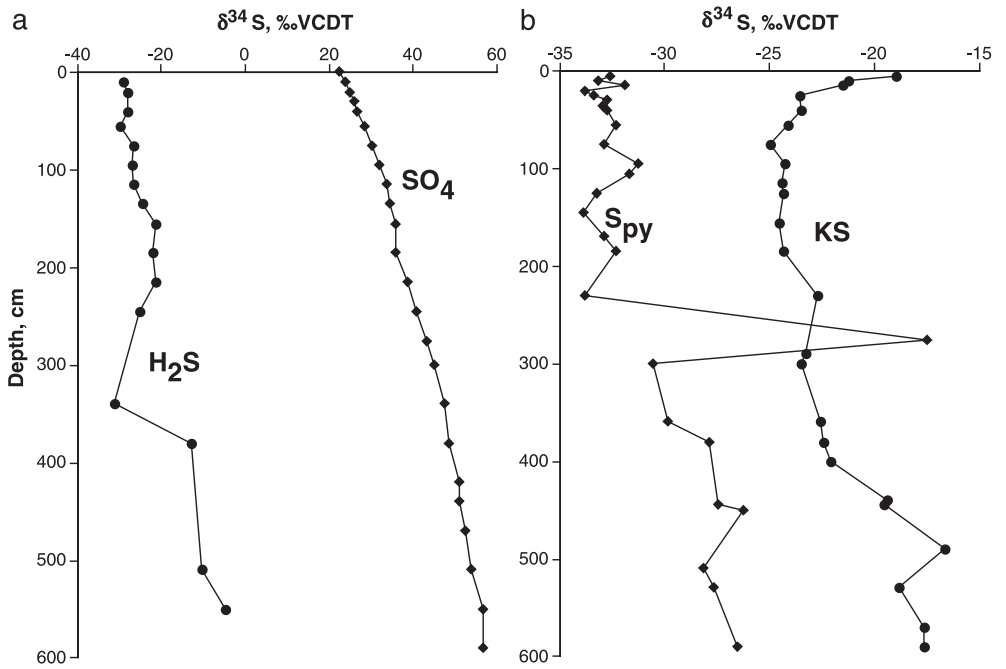

Fig. 4. Depth profiles of the sulfur isotope composition of (a) pore-water sulfate and sulfide; and (b) solid phase pyrite sulfur and kerogen sulfur in Cariaco Basin sediments.

in the ratio of KS to TOC should represent elevated accumulations of sulfur.

3. Results

3.1. Pore-water sulfur

Pore-water sulfate concentration is >25 mM in the surface sediments (compared to a value of ~29 mM for sea water) and decreases systematically to <5 mM at 600 cm depth in the sediments (Fig. 3). Pore-water sulfide concentration increases from approximately 0.1 mM at the sediment–water interface (SWI) to a maximum of ~8 mM at 250 cm depth and then decreases gradually to values near 0 mM at 6 m (Fig. 3). The pore-water (ZnS) aliquots were stored for ~3 years and suffered minor amounts of evaporation, and possibly oxidation, during that time. As a result, there is scatter in the data beyond that expected in the natural system. A smoothed curve (3rd order polynomial) through the data, however, clearly shows magnitudes and trends in sulfide concentrations that are typical of diagenetic profiles.

Pore-water sulfate and sulfide were analyzed for their sulfur isotope compositions ($\delta^{34}S_{SO_4}$ and $\delta^{34}S_{H_2S}$, respectively). $\delta^{34}S_{SO_4}$ increased from ~+22.8‰ (relative to a value of ~+21‰ for sea water, Rees et al., 1978; Böttcher et al., 2000) at the SWI to +57.6‰ at 600 cm sediment depth (Fig. 4). $\delta^{34}S_{H_2S}$ ranges from a low of −28.9‰ at the SWI (consistent with bottom water $\delta^{34}S_{\Sigma H_2S}$ values of −31‰ measured by Fry et al., 1991) to a maximum of −4.5‰ at 550 cm sediment depth. Although there is a trend of generally increasing $\delta^{34}S_{H_2S}$ with depth, there is a suggested excursion towards lighter isotope values below ~215 cm, reaching a depletion greater than the surface sediments of −30.9‰. There is an offset observed between pore-water sulfate and pore-water sulfide of 53.1‰ to 65.0‰ (78.9‰ in the $\delta^{13}S_{H_2S}$ excursion).

3.2. Sedimentary iron and sulfur accumulation

S_{py} concentration is 1.3 wt.% in surficial sediments and increases gradually to 1.5 wt.% at 350 cm depth (Fig. 3). Below ~350 cm, S_{py} concentration decreases to ~0.9 wt.% and then increases to >1.75 wt.% at ~6 m. Trends in reactive iron (Fe_R) concentration closely track those of S_{py}, increasing from surficial values of 1.25 wt.% to almost 1.6 wt.% with increasing depth. Like S_{py}, Fe_R concentration abruptly decreases at 350 cm to below 1 wt.% and increases again near 6 m sediment depth (Fig. 5).

Sedimentary concentrations of organic sulfur are discussed in terms of kerogen sulfur (KS) because a high resolution data set was obtained for KS, and differences between total organic sulfur and kerogen sulfur are minimal (less than analytical error in most samples). KS concentrations show a clear trend of increasing concentration with depth from 0.3 wt.% at the surface to 0.65 wt.% at 400 cm below the SWI (Fig. 3). KS concentration then decreases to values of almost 0.3 wt.% between ~400 and 575 cm, after which the concentration increases to almost 0.7 wt.%. The minimum concentration values of all

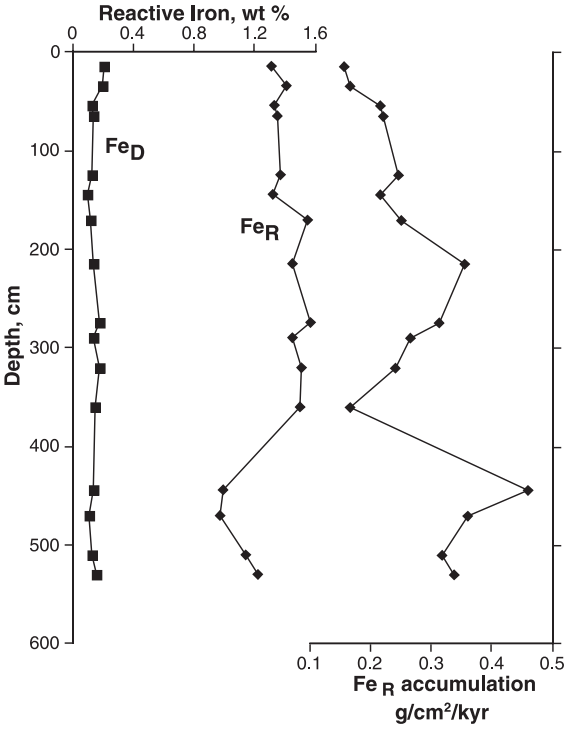

Fig. 5. Depth trends of Fe_R and Fe_D concentrations and Fe_R accumulation showing small and uniform contribution of diathianite iron, indicating reactive iron limitation for pyrite formation.

sulfur species and Fe_R at 450 cm is believed to reflect in part dilution due to increases in bulk sedimentation rate that occurred during deposition of this interval (e.g., Shipboard Scientific Party, 1997; Werne et al., 2000b).

Accumulations of S_{py} range from a low of ~ 0.15 g S/cm^2/ky in surface sediments to >0.4 g S/cm^2/ky at ~ 600 cm, the deepest sediments analyzed (Fig. 6). Between 300 and 450 cm, there is an excursion towards lower accumulations, reaching values < 0.2 g S/cm^2/ky. Reactive iron trends vary similarly, from a surface low of 0.15 g Fe/cm^2/ky to a deep maximum of ~ 0.45 g Fe/cm^2/ky, with an excursion toward lower values at ~ 350 cm reaching 0.15 g Fe/cm^2/ky (Fig. 5). KS accumulation is more variable but generally increases from essentially no accumulation at the surface sediments to a maximum of more than 0.2 g S/cm^2/ky at 450 cm; KS accumulation also shows an excursion to lower values (less than 0.1 g S/cm^2/ky) around ~ 350 cm (Fig. 6).

3.3. Sedimentary sulfur isotope trends

The $\delta^{34}S$ value for pyrite ($\delta^{34}S_{py}$) is − 33.8 ‰ in surface sediments (Fig. 4) and increases linearly with some scatter down core to a maximum of − 26.5 ‰ at 600 cm. $\delta^{34}S_{KS}$ values decrease significantly in near-surface sediments from − 18.9 ‰ at the SWI to − 25.0 ‰ at 50 cm and then increases gradually with depth to values of − 17.6 ‰ at 600 cm depth (Fig. 4). The sulfur isotope compositions of TOS and PBS were measured for five samples for comparison to the $\delta^{34}S_{KS}$ results. The overall trends are very similar. $\delta^{34}S_{TOS}$ ranges from − 24.9 ‰ at 50 cm to − 18.0 ‰ at 550 cm (Fig. 7). $\delta^{34}S_{PBS}$ is generally consistently depleted relative to TOS and KS by 2–3 ‰, ranging between approximately − 29.4 ‰ and − 20.5 ‰ (Fig.

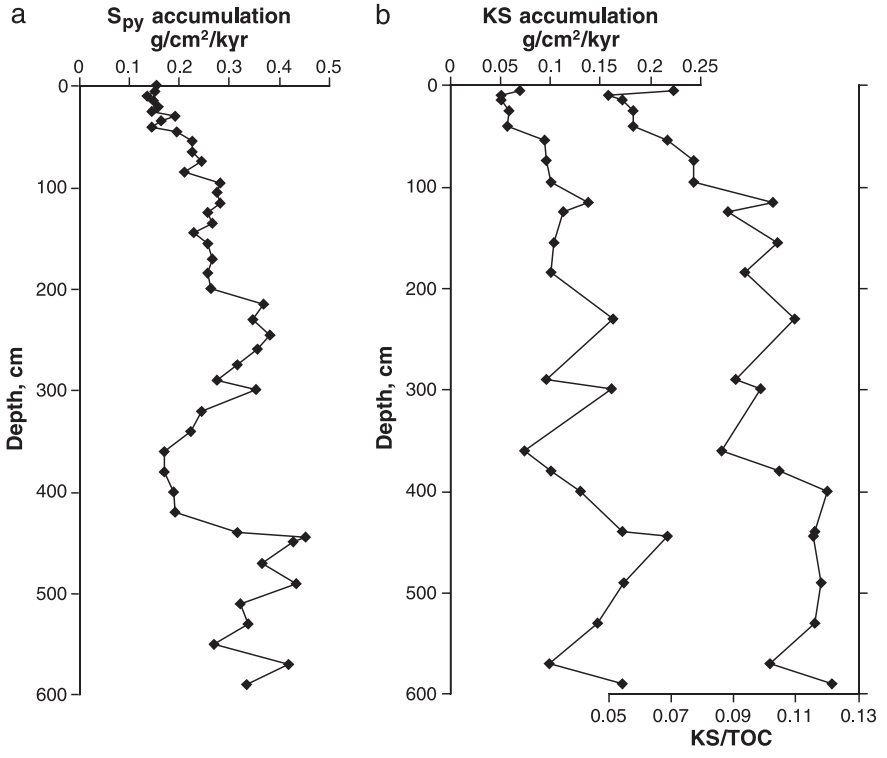

Fig. 6. (a) Depth profile of S_{py} accumulation. (b) Depth profiles of KS accumulation and the ratio KS/TOC, showing changes in the deposition of reduced sulfur in Cariaco Basin sediments.

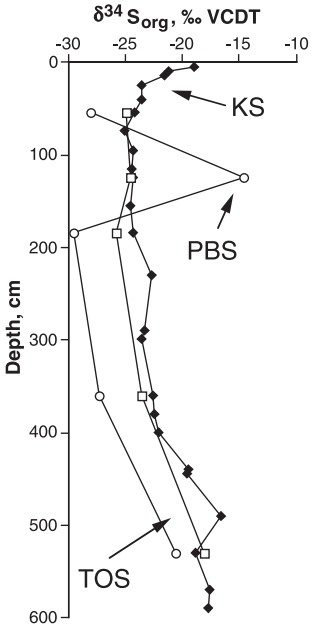

Fig. 7. Depth profiles of the sulfur isotope composition of different organic sulfur species (TOS, KS, and PBS) in Cariaco Basin sediments.

7). One point on the $\delta^{34}S_{PBS}$ curve is significantly enriched relative to the others (-14.5‰); however, the PBS analyses were only run on single samples from each interval due to small sample size. A slight enrichment in TOS relative to KS is observed in the same interval, so it is possible that this is a real value.

4. Discussion

4.1. Sulfate reduction and anaerobic sulfide oxidation

The decrease in pore-water sulfate concentrations with depth (Fig. 3), indicates the occurrence of bacterial sulfate reduction in the sediments. The decrease in pore-water sulfide concentration in the lower part of the interval suggests Fe-sulfide formation and/or OM sulfurization. The pore-water sulfur isotope trends ($\delta^{34}S_{SO_4}$ and $\delta^{34}S_{H_2S}$) indicate a sedimentary system that is restricted (Hartmann and Nielsen, 1969; Zaback et al., 1993; Lyons, 1997)—i.e., the pore-water sulfate and sulfide are not able to diffuse freely through the vertical sequence of sediments relative to their rates of consumption via bacterial sulfate reduction, organic matter sulfurization, and pyrite formation. The observed downcore increase in $\delta^{34}S_{\Sigma H_2S}$ would be exacerbated by an integrated history of sulfide removal through reactions to form pyrite and OSC. The negative excursion observed in the pore-water sulfur isotopic data ($\delta^{34}S_{H_2S}$) between $\sim$250 and 350 cm could result from a number of different processes. One likely possibility is that the $\delta^{34}S_{H_2S}$ excursion is due to a decrease in the amount of diagenetic pyrite formed at that horizon due to extreme Fe_R limitation (cf. Fig. 5; decrease in Fe_R accumulation at $\sim$350 cm coeval with the negative excursion in $^{34}S_{H_2S}$). Such a decrease in pyrite formation would lead to a relatively larger proportion of early formed pore-water sulfide in restricted sediments such as those in the Cariaco Basin.

A large offset is observed between the sulfur isotope composition of pore-water sulfate and pore-water sulfide throughout the interval investigated—generally 50–65‰. Such a large difference is more than has ever been observed as a result of bacterial sulfate reduction alone (Habicht and Canfield, 1997, 2001; Brüchert et al., 2001; Canfield, 2001; Detmers et al., 2001) with the exception of one study in the deep subsurface in which a fractionation of 72‰ was observed (Wortmann et al., 2001). It has been proposed that the most likely mechanism for sulfur isotope fractionations between sulfate and sulfide on the order of those observed in the Cariaco Basin sediments is partial oxidation of sulfide to reactive intermediates such as elemental sulfur, thiosulfate, and sulfite followed by microbial disproportionation to sulfate and sulfide (Jørgensen, 1990; Canfield and Thamdrup, 1994; Canfield et al., 1998b; Habicht et al., 1998; Böttcher et al., 2001). There is a minimal sulfur isotope fractionation associated with sulfide oxidation, but a significant sulfur isotope fractionation has been observed associated with disproportionation of elemental sulfur, thiosulfate, and sulfite, thus, cycling between sulfide and reactive intermediates via oxidation and disproportionation is believed to be responsible for sulfide isotopic depletion in excess of that attributable to bacterial sulfate alone (Canfield and Thamdrup, 1994; Canfield et al., 1998b; Habicht et al., 1998; Böttcher et al., 2001). There is laboratory evidence for sulfide oxidation and disproportionation

occurring under anoxic conditions (Bak and Cypionka, 1987; Fry et al., 1985, 1988; Böttcher and Thamdrup, 2001; Böttcher et al., 2001). Evidence also exists for partial oxidation and disproportionation in natural anoxic systems (Thamdrup et al., 1994; Böttcher et al., 1998b; Zopfi et al., 2001). However, these systems all have the potential for anaerobic phototrophic sulfide oxidation and/or the availability of other oxidants such as Fe or Mn (oxy)hydroxides.

In the Cariaco Basin, it is likely that sulfide oxidation and subsequent disproportionation of reactive intermediates such as elemental sulfur, polysulfides, and thiosulfate take place in the chemocline in the water column where both oxygen and sulfide are available, and thiosulfate has been detected (Fry et al., 1985). The observed fractionation between sulfate and sulfide increases with depth in the Cariaco sediments, however, suggesting either that the processes of partial oxidation of sulfide and subsequent disproportionation of intermediates is continuing in the sediments, or that sulfur isotope fractionation associated with sulfate reduction was greater in the past than it is today, leading to a larger observed fractionation with increasing with depth. Both of these possible interpretations have significant problems, however. It seems unlikely that pore-water sulfate and sulfide S-isotope profiles would be preserved in sediments for 10,000 years (e.g., to maintain a large offset between $\delta^{34}S_{SO_4}$ and $\delta^{34}S_{H_2S}$), which would be required in order for a greater rate of sulfate reduction in the past to explain the observed trend. Partial oxidation of sulfide in the Cariaco Basin sediments is also problematic, however, due to the lack of oxidants. The sediments are deeply removed from both the photic zone and the chemocline, so photo-oxidation and chemocline-related oxidation are not possible. Reactive oxides (such as Fe and Mn (oxy)hydroxides) are also in very limited supply (Lyons et al., 2003, this volume).

Therefore, we propose that sulfide oxidation and disproportionation of elemental sulfur, thiosulfate, and sulfite may be carried out by microbes living both anaerobically and aphotically, either as heterotrophs or chemoautotrophs, utilizing a currently unknown sulfide-oxidation pathway. Support for this hypothesis is provided in a recent study by Madrid et al. (2001). In this study, 16S rRNA gene sequences of ε-proteobacteria were identified in sediment traps in the deep water column of the Cariaco Basin which they propose are anaerobic autotrophic sulfide-oxidizing bacteria (Madrid et al., 2001).

4.2. Pyrite accumulation in euxinic sediments

The general downcore increase in pyrite sulfur concentrations in surficial Cariaco sediments suggests contributions from both syngenetic and diagenetic pyrite, assuming surficial sediment S_{py} concentrations can be interpreted as deriving solely from syngenetic pyrite formation (which is supported by surficial sediment $\delta^{34}S_{py}$ values, see discussion below). Between 350 and 550 cm, however, there is a significant decrease in S_{py} concentration to values below 1.0 wt.%. A decrease in pyrite formation of this magnitude (i.e., to levels lower than present-day syngenetic pyrite formation) suggests the possibility of a major reorganization of the processes that contribute to pyrite formation; however, it is also possible that the decrease in S_{py} concentration is an artifact of changing dilution ratios resulting from elevated inputs of non-Fe bearing biogenic silica and carbonate.

S_{py} accumulation in surficial sediments is interpreted to represent the deposition of syngenetic pyrite, and the increase in accumulation with depth is interpreted as the continuous diagenetic addition of pyrite to the sedimentary system. The trend of S_{py} accumulation is similar to that for S_{py} concentration; however, the shift to decreased values is limited to between ~ 350 and 450 cm depth (Fig. 6), rather than extending to 550 cm as does S_{py} concentration (Fig. 3). It is of importance that the decrease in S_{py} accumulation rate at depth does not reach values below the surficial sediments, in contrast to the S_{py} concentration. This observation suggests that indeed accumulations may be a more accurate record of actual syngenetic and diagenetic pyrite deposition in the Cariaco Basin than concentrations and may be useful in other environments with appreciable variations in biogenic and detrital sedimentation.

4.3. Reactive iron limitation

The availability of reactive iron species is known to be a fundamental limitation on the formation of pyrite, particularly in euxinic environments (Canfield, 1989; Canfield et al., 1992, 1996). In a system that is iron limited, sulfide that remains in the pore-waters

(i.e., is not consumed by pyrite formation) is available for incorporation into organic matter. Because pyrite formation is kinetically favored relative to organic matter sulfurization, iron-limited pyrite formation is an important precondition for significant OM sulfurization. In the Cariaco Basin sediments, numerous lines of evidence indicate iron limitation with respect to pyrite formation. Because the Fe-limited nature of pyrite formation in the Cariaco Basin is discussed in detail in Lyons et al. (2003, this volume), only a brief summary is provided here.

The depth trends for S_{py} and Fe_R both exhibit sudden decreases between ~350 and 550 cm depth in the sediments (Figs. 5 and 6), which is consistent with Fe limitation in combination with bulk sedimentary dilution by non-iron-bearing biogenic phases. Concentrations of dithionite extractable iron (Fe_D; data from Raiswell and Canfield, 1998) are extremely low and uniform throughout the interval of study (Fig. 5), indicating that nearly all the available Fe has been used in pyrite formation. Furthermore, the persistence of high concentrations of pore-water sulfide provides further evidence for iron limitation.

4.4. Isotope constraints on sulfur deposition: syngenetic vs. diagenetic pyrite formation

The potential for pyrite to form in either the sediments (diagenetically), water column (syngenetically), or both makes it difficult to constrain the timing of pyrite formation, which in turn makes it more difficult to assess the impact of pyrite formation on the formation of organic sulfur. It is important to know the relative contributions of syngenetic and diagenetic pyrite because the process of pyrite formation competes directly with that of OM sulfurization for available sulfide. Recent studies in the Black Sea have indicated that the sulfur isotope signature of syngenetically formed pyrite is typically isotopically light compared to that of diagenetically formed pyrite due to the larger reservoir of dissolved sulfide in the relatively open system of the water column as opposed to the restricted system of the pore-waters (Calvert et al., 1996; Lyons, 1997). Not all sedimentary deposits act as restricted systems with respect to dissolved sulfate/sulfide diffusion (e.g., Jørgensen, 1977); however, diffusion of dissolved sulfur species in such environments is likely to be enhanced by bioturbation, which is not a significant factor in the laminated sediments of the Cariaco Basin.

In the Cariaco Basin, there is evidence for the formation of both syngenetic and diagenetic pyrite. $\delta^{34}S_{py}$ values display a trend of increasing isotope enrichment with depth (Fig. 4). The values above ~200 cm are all depleted relative to pore-water sulfide (~ -34‰ compared to -30‰ for pore-water sulfide), suggesting that the majority of the pyrite in the upper sediments formed in the water column under relatively open system conditions and that any diagenetic pyrite forming in near surface sediments was isotopically depleted relative to deeper forming diagenetic pyrite. Below 200 cm, $\delta^{34}S_{py}$ values increase to ~ -26‰, as would be expected if pyrite were continuing to form diagenetically under increasingly restricted conditions in deeper sediments.

Because we have the sulfur isotope composition of both pyrite and pore-water sulfide, as well as the concentration and accumulation of pyrite, we should be able to use an isotopic mass balance equation to model the isotope composition of syngenetic and diagenetic pyrite. First, we must determine the relative concentration of both syngenetic and diagenetic pyrite. Because of the potential for diluting effects, we have used pyrite accumulations in place of concentration. To determine the relative accumulations of syngenetic and diagenetic pyrite, we make the assumption that the accumulation of pyrite averaged over the upper few cm represents the average input of syngenetic pyrite; diagenetic pyrite accumulation is calculated as the difference between the total pyrite accumulation and the average value chosen to represent syngenetic contributions. This assumption requires that there has been no significant change in the accumulation rate of syngenetic pyrite over time, which may not be correct as will be demonstrated below. However, this is a good first order approximation. If we therefore assume constant syngenetic pyrite accumulation over the last 12 ^{14}C ky to be 0.15 g/cm^2/ky, the diagenetic pyrite accumulations range from 0.00 g/cm$_2$/ky in the surface sediments to 0.30 g/cm^2/ky in the deepest sediments, suggesting that diagenetic pyrite may account for between 50% and 75% of the pyrite in the deeper sediments (Fig. 8a) (compare Lyons et al., 2003, this volume).

The sulfur isotopic signature of sedimentary pyrite should provide a test of whether the assumptions used

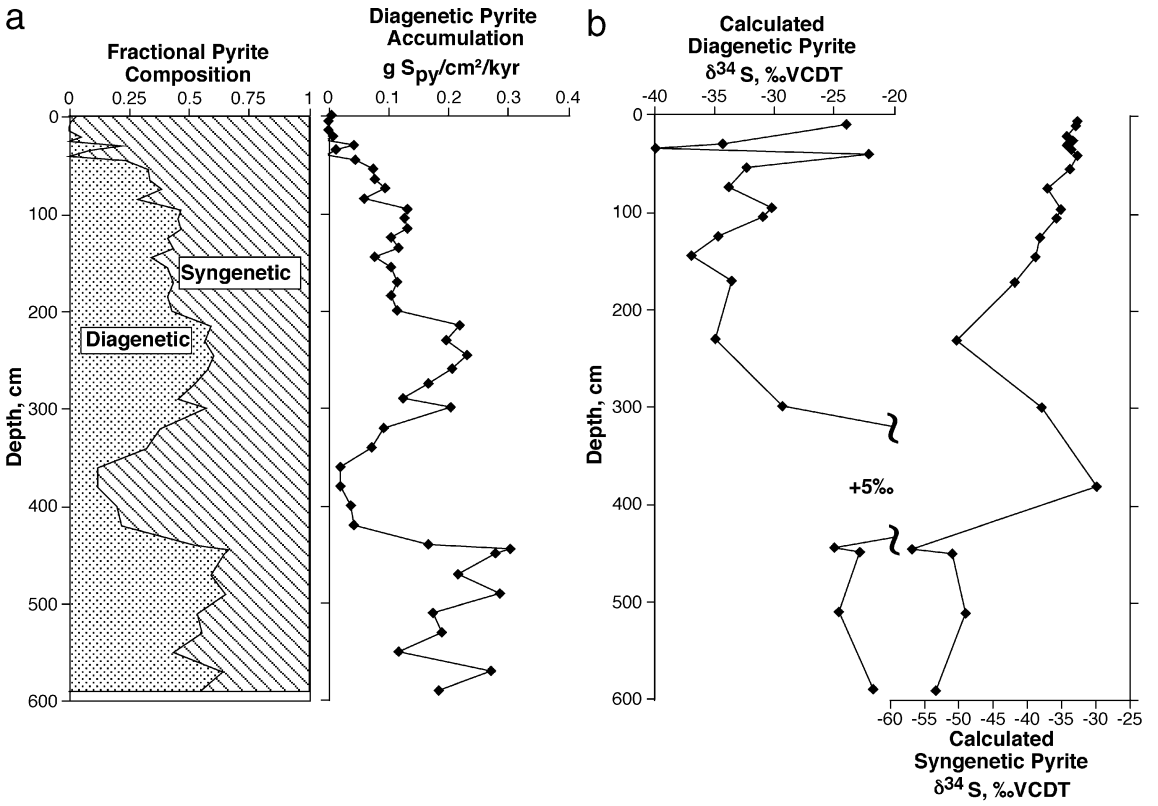

Fig. 8. (a) Depth trends of diagenetic and syngenetic pyrite accumulation. Diagenetic pyrite calculated assuming that syngenetic input was constant and represented by the pyrite concentration in the upper 50 cm. (b) Depth trends of sulfur isotope compositions of diagenetic and syngenetic pyrite calculated using weighted isotopic mass balance.

in the calculation of the diagenetic fraction of the pyrite are valid. We can apply a simplified isotope mass balance equation:

$$\delta_1 A_1 + \delta_2 A_2 = \delta_3 A_3,$$

where δ_1, δ_2, and δ_3 represent the isotope composition of syngenetic, diagenetic, and total pyrite, respectively, and A_1, A_2, and A_3 represent their accumulations. This approach allows us to calculate the theoretical sulfur isotope composition of diagenetic pyrite if we assume that the syngenetic pyrite and the pyrite in the surface sediment layers has a S-isotope composition similar to bottom water sulfide ($\sim -31‰$, Fry et al., 1991). We have chosen a δ^{34}S value of $-32‰$ for syngenetic pyrite because it is between the value of bottom water sulfide and pyrite in surficial sediments. Based on these assumptions and using the accumulation rates and δ^{34}S values measured on total pyrite, the calculated isotope composition of diagenetic pyrite is insignificantly different from total pyrite in the upper 250 cm of the sediments and is enriched relative to total pyrite by $\sim 5‰$ in the deeper sediments (Fig. 8b). There is a gradual downcore ^{34}S enrichment similar to that of total pyrite, as would be expected for pyrite formation under restricted pore-water conditions. One point at 380 cm lies significantly off the trend, which we believe to be an artifact of the accumulation and mass balance approach.

Alternatively, we can calculate the δ^{34}S of syngenetic pyrite by first assuming that diagenetic pyrite in any depth interval has the same δ^{34}S as present-day coeval pore-water sulfide (as measured in this study). It should be noted that the δ^{34}S of diagenetic pyrite at any interval truly reflects an integrated record of the

$\delta^{34}S$ of pore-water sulfide throughout the period of diagenetic pyrite formation. However, given the possibility that pore-water sulfide profiles have changed through time, particularly given the changing TOC concentrations and sedimentation rates, this assumption is a reasonable first order approximation of the $\delta^{34}S$ of diagenetic pyrite. Based on these assumptions and using the measured total pyrite accumulations and $\delta^{34}S_{py}$ as before, the theoretical $\delta^{34}S$ of syngenetic pyrite is calculated (Fig. 8b). The $\delta^{34}S$ of syngenetic pyrite in surficial sediments is consistent with the bottom water value of $-31‰$ (Fry et al., 1991), as expected given the assumption that all pyrite in the most surficial sediments is syngenetically formed, and generally trends towards more ^{34}S depleted values with increasing depth.

If the calculated $\delta^{34}S$ values of syngenetic pyrite are accurate, it is possible that the lower $\delta^{34}S$ of syngenetic pyrite in deeper sediments resulted from enhanced microbial recycling of dissolved sulfur species in the chemocline. Evidence exists for a substantially increased accumulation rate of organic carbon in the deeper sediments (Werne et al., 2000b). Such an increase in the production of organic matter in the water column would stimulate higher rates of bacterial sulfate reduction, producing more sulfide. Though higher rates of sulfate reduction alone could lead to more ^{34}S enriched sulfide (Habicht and Canfield, 1997; Brüchert et al., 2001; Canfield, 2001), the concomitant increase in the amount of sulfide oxidation and subsequent disproportionation reactions of intermediate reactive species such as elemental sulfur, thiosulfate, and sulfite could lead to much more ^{34}S depleted bottom-water sulfide (cf. Fry et al., 1988; Jørgensen, 1990; Canfield and Thamdrup, 1994; Canfield et al., 1998b; Habicht et al., 1998; Böttcher et al., 2001, Böttcher and Thamdrup, 2001), as recorded in the syngenetic pyrite.

Between $\sim$ 235 and 450 cm, the calculated $\delta^{34}S$ of syngenetic pyrite is considerably enriched. This ^{34}S enrichment may be an artifact of the extremely low pyrite accumulations that occurs at the same horizon, due in part to changing bulk sedimentation rates. Such artifacts illustrate the weakness of this type of calculation; however, the overall trends of the theoretically calculated values of both $\delta^{34}S$ of syngenetic pyrite and $\delta^{34}S$ of diagenetic pyrite do appear to be explainable and consistent with what is known of the depositional system in the Cariaco Basin. The sediments of the Cariaco Basin, like all marine sediments, are fundamentally a non-steady-state system, and variations in the depositional conditions over thousands of years result in a complicated geochemical signature (see also Lyons et al., 2003, this volume).

4.5. Organic sulfur accumulation in euxinic sediments

The trend of increasing organic sulfur concentration with depth (Fig. 3) suggests either that more organic sulfur was being deposited as primary OM in the past or that sulfurization of OM has been occurring over the past 12 ^{14}C ky. Because primary OM has a relatively small concentration of sulfur (e.g., Chen et al., 1996) which is predominantly present in the most labile forms of OM (i.e., proteins), and because diagenetic sulfurization of OM was unambiguously identified in Cariaco sediments (Werne et al., 2000a), we propose that the increasing concentrations of organic sulfur with increasing depth indicate diagenetic additions of sulfur to sedimentary OM rather than an increase in the deposition rate of primary biosulfur at that time. KS accumulation and KS/TOC also generally increase with depth, supporting the hypothesis of progressive diagenetic sulfurization of OM in the sediments. The isotope compositions of TOS, KS, and PBS all generally increase with depth (Fig. 7), supporting the interpretation that diagenetic sulfurization is continuing with depth and that the sulfur being incorporated into OM is derived ultimately from pore-water sulfide in an integrated fashion.

One aspect of the KS accumulation and KS/TOC curves that merits further discussion is the excursion to lower values just below 300 cm. This is the same horizon that shows significant decreases in S_{py} accumulation, Fe_R accumulation, and $\delta^{34}S_{\Sigma H_2S}$. The simultaneous decreases in S_{py} and KS accumulations suggest that at the time of deposition of that horizon ($\sim$ 8–9 ^{14}C ky), little sulfide was being incorporated into either pyrite or OM.

4.6. Isotope constraints on the timing and pathway(s) of OM sulfurization

The timing and pathways of OM sulfurization have historically proven difficult to constrain. Recent studies have demonstrated that, at least in some environ-

ments, OM sulfurization can occur during very early diagenesis—i.e., the first several hundred to several thousand years (e.g., Wakeham et al., 1995; Kok et al., 2000b; Werne et al., 2000a). The recent identification of an almost quantitative conversion of malabaricatriene to a triterpenoid thiane over 10 ky in the Cariaco Basin (Werne et al., 2000a) provides real constraints on the timing of OM sulfurization, at least for this particular compound. The presence of highly branched isoprenoid (HBI) thiophenes and thiolanes in surficial sediments of the Cariaco Basin (where the triterpenoid thiane has not yet formed; Werne et al., 2000a) and the Black Sea (Wakeham et al., 1995) suggests earlier, more rapid sulfurization (e.g., completed in $\sim$ 3000 years). However, the presence of unreacted functionalized lipids at depths below complete conversion of malabaricatriene to triterpenoid thiane in the Cariaco Basin (Werne et al., 2000a,b) suggests the possibility of much slower sulfurization rates.

The isotope data we have for pore-water sulfide, if combined with the timing of the sulfurization reaction identified in Werne et al. (2000a), should allow us to predict the sulfur isotope composition of the resulting triterpenoid thiane by using weighted isotope mass balance equations. Comparison of the predicted values with measured values of the sulfur isotope composition of the different pools of organic sulfur should subsequently allow us to place constraints on the timing and possible pathways of OM sulfurization. In addition, we should be able to predict the sulfur isotope composition that would result from OM sulfurization reactions of different rates using similar integrated, weighted isotope mass balance equations.

If we assume that the sulfur being incorporated into sedimentary OM is derived directly from coeval pore-water sulfide with no isotope fractionation and is added continuously with depth, we can use equations of the generalized form:

$$\delta_1 R_1 + \delta_2 R_2 + \ldots + \delta_n R_n = \delta_N R_N,$$

where δ_n represents the sulfur isotope composition of pore-water sulfide at depth n, R_n represents the fraction of the initial precursor compound sulfurized at depth n, δ_N represents the sulfur isotope composition of the organic sulfur integrated from depth 0 to depth n, and R_N represents the total fraction of sulfurized triterpenoid at depth N. This approach allows us to predict the theoretical sulfur isotope composition of the triterpenoid thiane ($\delta^{34}S_{TT}$) as it becomes sulfurized with increasing depth in the sediments (integrated over the entire depth of sulfur incorporation). The problems associated with the variations in sedimentation rate can be circumvented by utilizing a ratio of the reacted to unreacted triterpenoid (e.g., the ratio of the precursor compound, A, to the sum of the precursor and product compounds, A + B). To extend this calculation to bulk OS (e.g., TOS, KS, and PBS), we have used sulfurization rates for three reactions (Fig. 9a): a fast reaction (e.g., completed in <3 ky) such as may occur for HBI thiophenes/thiolanes in the Black Sea (Wakeham et al., 1995) and Cariaco Basin (Werne et al., 2000a), an "average" reaction such as the malabaricatriene to triterpenoid thiane conversion in Werne et al. (2000a), and a slow reaction (e.g., completed in $\sim$ 12 ky) such as may be occurring in deeper sediments of the Cariaco Basin (e.g., >6 m).

The theoretically predicted sulfur isotope values of organic sulfur ($\delta^{34}S_{Th}$) display trends of increasing

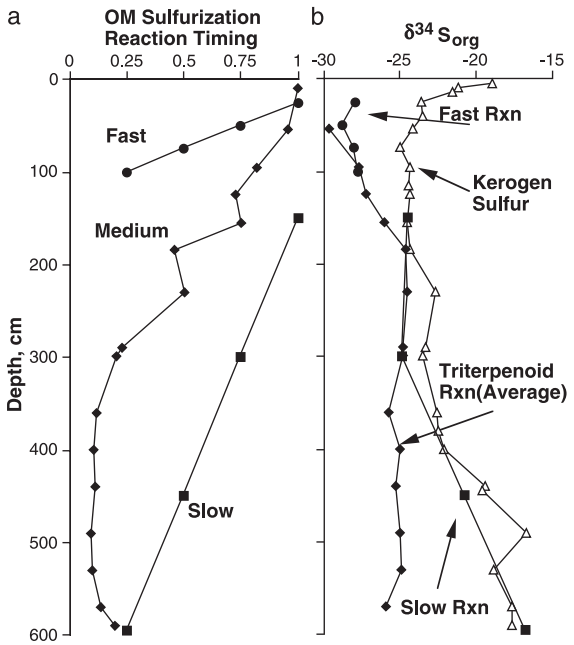

Fig. 9. (a) Illustration of theoretical OM sulfurization reactions, showing fast, medium, and slow reaction timing. (b) Depth profile of theoretically predicted $\delta^{34}S_{Th}$ compared to measured $\delta^{34}S_{KS}$.

isotope enrichment with depth as a result of the increasing $\delta^{34}S_{\Sigma H_2S}$ values (Fig. 9b). Above ~200 cm, the theoretical isotope compositions are depleted relative to the measured $\delta^{34}S_{KS}$ values by almost 10‰. Deeper $\delta^{34}S_{Th}$ values are very similar to $\delta^{34}S_{KS}$ values. The isotope enrichment of $\delta^{34}S_{KS}$ relative to the theoretically calculated values in the upper ~200 cm can be explained either by the delivery of ^{34}S-enriched primary organic sulfur or through the existence of a kinetic isotope affect associated with extremely rapid OM sulfurization in the near-surface sediments. Although neither of these two possibilities can be unequivocally excluded based on the existing data, the similarities between the $\delta^{34}S_{Th}$ and the measured $\delta^{34}S_{PBS}$ at 50 cm (Figs. 9b and 7) suggest that the newly produced organic sulfur in surface sediments is depleted in ^{34}S, but the kerogen sulfur is isotopically enriched in surface sediments due to a relatively greater component of ^{34}S-enriched biogenic sulfur delivered with primary OM.

The sulfur isotope composition of primary OM (i.e., not diagenetically added sulfur) is typically similar to dissolved sulfate as a result of the small fractionation associated with assimilatory sulfate reduction (Kaplan et al., 1963; Chambers and Trudinger, 1979).

If we assume that the isotope composition of primary bio-sulfur is +20‰ (cf. Kaplan et al., 1963; Goldhaber and Kaplan, 1974; Rees et al., 1978; Chambers and Trudinger, 1979; Canfield et al., 1998a; Böttcher et al., 2000), it would only take a small proportion of bio-sulfur to shift the sedimentary $\delta^{34}S_{TOS}$ to more enriched values. In fact, a simple mass balance calculation based on the assumptions that (1) primary bio-sulfur is +20‰, (2) early diagenetic organic sulfur is −30‰ (the value of surficial pore-water sulfide), and using a measured $\delta^{34}S_{KS}$ value of −18‰ for organic sulfur at the SWI indicates that approximately 25% of the organic sulfur in surficial sediments is primary bio-sulfur. However, primary bio-sulfur is believed to occur predominantly as highly labile compounds and would therefore tend to be rapidly remineralized in surface sediments and/or the water column, as is suggested by the sharp decrease in $\delta^{34}S_{KS}$ in the upper 50 cm of the sediments. Therefore, although bio-sulfur is a minor proportion of the total organic sulfur pool, it is possible that the enrichment in TOS relative to S_{py} is due in part to preservation of primarily deposited bio-sulfur in sediments.

The fact that TOS, KS, PBS, and the theoretically predicted OS are all isotopically enriched relative to pyrite supports the hypothesis that organic sulfur is indeed forming during later diagenesis than pyrite, as expected given the relative reactivities of Fe and OM towards H_2S (Gransch and Posthuma, 1974; Hartgers et al., 1997). The consistent offset between $\delta^{34}S_{py}$ and $\delta^{34}S_{TOS}$ also suggests the possibility of differences in sulfur isotope fractionations in the formation pyrite and organic sulfur, but whether these differences are related to the source of sulfur or the specific formation pathways remains unclear. The similarities between the $\delta^{34}S_{Th}$ values and the $\delta^{34}S_{TOS}$ values with increasing depth suggest that sulfur incorporated into OM during early diagenesis is derived primarily from pore-water sulfide or an intermediate derived from partial sulfide oxidation, and that there is not a significant fractionation associated with this uptake.

4.7. Comparison with other sulfur rich systems

The relative isotope trends identified in the Cariaco Basin sediments ($\delta^{34}S_{py}$, $\delta^{34}S_{TOS}$, $\delta^{34}S_{\Sigma H_2S}$) are generally similar to those identified in other euxinic sediments. For example, trends in Peru Margin sediments (Mossman et al., 1991) are very similar to those in the Cariaco Basin, although the depth interval over which these analagous trends occur is significantly different, and the absolute isotope values are more depleted in ^{34}S in the Cariaco Basin than in the Peru Margin. The consistently more depleted sulfur isotope compositions in the Cariaco sediments may be a result of the increased relative size of the water-column sulfide reservoir due to the increased intensity of euxinic conditions in the Cariaco Basin as compared to the Peru Margin, which may not have been euxinic over the interval of study. The depleted sulfur could also be attributed simply to a greater component of syngenetic pyrite in Cariaco sediments. Another possibility is the existence of a more active microbial recycling of sulfide in the Cariaco Basin compared to the Peru Margin, which would be expected with sulfide in the water-column. Despite differences in magnitudes and stratigraphic scales, the similarities in the relative trends of $\delta^{34}S_{Spy}$, $\delta^{34}S_{TOS}$, and $\delta^{34}S_{\Sigma H_2S}$ with depth suggest that the processes occurring in

both environments are fundamentally the same. The different depth scales over which these processes are occurring, however, suggest fundamental differences in the rates of sedimentation, pyrite formation, OM sulfurization reactions, and sedimentary microbial sulfur cycling. These differences are all linked to the relative availability of reactive species, such as water column and pore-water sulfide; intermediate sulfur species such as elemental sulfur, thiosulfate, and sulfite; as well as iron monosulfides and reactive iron. Indeed, similar relative trends are observed in a number of other systems, such as the Miocene Monterey Formation (Zaback and Pratt, 1992), St. Andrew Bay, Florida (Brüchert and Pratt, 1996), and a number of others (see Anderson and Pratt, 1995).

5. Conclusions

The concentrations, accumulations, and isotope compositions of several different species of organic and inorganic sulfur have been determined in euxinic sediments from the Cariaco Basin, including pore-water sulfide and sulfate, pyrite, total organic sulfur, kerogen sulfur, and polar bitumen sulfur. Weighted isotope mass balance calculations have been used to estimate the different contributions of syngenetic and diagenetic pyrite to the sediments. Results suggest that the relative contributions have varied over the last 12 ^{14}C ky, with generally greater relative contributions of diagenetic pyrite in older sediments, as would be expected given their longer burial history.

An excursion to lower diagenetic pyrite accumulations is observed in sediments deposited approximately 9–10 ^{14}C ky ago at a horizon that is also marked by a significant change in bulk sedimentation rate. In addition, the deposition of syngenetic pyrite may have been significantly greater at times in the past, such as between $\sim$10 and 12 ^{14}C ky before present. It is proposed that the elevated contributions of syngenetic pyrite at that time are related to enhanced primary productivity in surface waters. The enhanced primary production drove elevated rates of bacterial sulfate reduction, providing a greater supply of dissolved sulfide in the water column, which could react with a potentially larger supply of reactive iron associated with increased delivery of clastic material (cf. Lyons et al., 2003, this volume). This supply of sulfide in the water column could also have driven enhanced microbial sulfide recycling at the chemocline, resulting in an even more depleted sulfur isotope signature of sulfide at that time. Such a depleted sulfide signature is suggested by the ^{34}S-depleted δ^{34}S values calculated for syngenetic pyrite in deeper sediments.

Organic sulfur isotope data suggest contributions of organic sulfur from both diagenetic sulfurization of OM and primary bio-sulfur in the Cariaco Basin, though the vast majority of the organic sulfur is diagenetically formed. Isotope trends suggest that OM sulfurization occurs continuously with increasing depth, imparting an increasingly ^{34}S-enriched sulfur isotope composition to organic sulfur. The theoretically predicted isotope composition of diagenetically added sulfur in OM is consistent with measured $\delta^{34}S_{TOS}$, $\delta^{34}S_{KS}$, and $\delta^{34}S_{PBS}$ values, suggesting that most of the sulfur incorporated into OM is ultimately derived from pore-water sulfide. Currently, however, it is not possible to determine whether the sulfur being incorporated into organic matter is pore-water sulfide or whether this incorporation occurs indirectly via reactive intermediates resulting from partial oxidation of sulfide (such as polysulfides or elemental sulfur).

The identification of a large offset between pore-water sulfate and pore-water sulfide (55–65 ‰) suggests the existence of microbially mediated sulfur recycling processes in the sediments, including partial oxidation of sulfide to elemental sulfur, thiosulfate, or sulfite followed by bacterial disproportionation of these reactive intermediate sulfur species (although the oxidation mechanism at depth in anoxic/sulfidic sediments with little or no reactive oxide species is poorly understood). While this is not a new conclusion, it does add evidence to the possibility of organic matter sulfurization via such reactive intermediates. Furthermore, the existence of such sulfide oxidation reactions in deep euxinic sediments suggests that microbes are living in the Cariaco Basin sediments that are capable of oxidizing sulfide anaerobically and aphotically, either as chemoheterotrophs or chemoautotrophs.

Acknowledgements

R. Murray and D.G. Pearson are thanked for their significant contributions to shipboard sediment pro-

cessing and pore-water data generation. We also thank ODP, particularly the Leg 165 Scientific Party, for providing samples, and especially thank M. Baas, K. Keel, J. Fong, S. Studley, and E. Elswick for technical assistance. Partial financial support was provided to TWL by JOI-USSSP, and to JPW by EAOG Travel Grant. Funds for facility development and research were also provided to TWL by NSF grants EAR-9875961 and EAR-9726264. **[EO]**

References

Adam, P., Philippe, E., Albrecht, P., 1998. Photochemical sulfurization of sedimentary organic matter: a widespread process occurring at early diagenesis in natural environments? Geochim. Cosmochim. Acta 62, 265–271.

Aizenshtat, Z., Stoler, A., Cohen, Y., Nielsen, H., 1983. The geochemical sulphur enrichment of recent organic matter by polysulfides in the Solar-Lake. In: Bjorøy, M., et al. (Eds.) Advances in Organic Geochemistry 1981. Wiley, New York, pp. 279–288.

Anderson, T.F., Pratt, L.M., 1995. Isotope evidence for the origin of organic sulfur and elemental sulfur in marine sediments. In: Vairavamurthy, M.A., Schoonen, M.A.A. (Eds.), Geochemical Transformations of Sedimentary Sulfur. ACS Symposium Series, vol. 612, pp. 378–396. Washington, DC.

Bak, F., Cypionka, H., 1987. A novel type of energy metabolism involving fermentation of inorganic sulphur compounds. Nature 326, 891–892.

Berner, R.A., 1970. Sedimentary pyrite formation. Am. J. Sci. 268, 1–23.

Berner, R.A., 1984. Sedimentary pyrite formation: an update. Geochim. Cosmochim. Acta 48, 605–615.

Berner, R.A., 1987. Models for carbon and sulfur cycles and atmospheric oxygen: application to Paleozoic geologic history. Am. J. Sci. 287, 177–196.

Berner, R.A., Raiswell, R., 1983. Burial of organic carbon and pyrite sulfur in sediments over Phanerozoic time: a new theory. Geochim. Cosmochim. Acta 47, 855–862.

Boesen, C., Postma, D., 1988. Pyrite formation in anoxic environments of the Baltic. Am. J. Sci. 285, 193–206.

Böttcher, M.E., Thamdrup, B., 2001. Anaerobic sulfide oxidation and stable isotope fractionation associated with bacterial sulfur disproportionation in the presence of MnO_2. Geochim. Cosmochim. Acta 65, 1573–1581.

Böttcher, M.E., Smock, A., Cypoinka, H., 1998a. Sulfur isotope fractionation during experimental precipitation of iron(II) sulfide and manganese(II) sulfide at room temperature. Chem. Geol. 146, 127–134.

Böttcher, M.E., Oelschläger, B., Höpner, T., Brumsack, H.-J., Rullkötter, J., 1998b. Sulfate reduction related to the early diagenetic degradation of organic matter and "black spot" formation in tidal sandflats of the German Wadden Sea (southern North Sea): stable isotope (^{13}C, ^{34}S, ^{18}O) and other geochemical results. Org. Geochem. 29 (5–7), 1517–1530.

Böttcher, M.E., Schale, H., Schnetger, B., Wallmann, K., Brumsack, H.-J., 2000. Stable sulfur isotopes indicate net sulfate reduction in near-surface sediments of the deep Arabian Sea. Deep-Sea Res., II 47, 2769–2783.

Böttcher, M.E., Thamdrup, B., Vennemann, T.W., 2001. Oxygen and sulfur isotope fractionation during anaerobic bacterial disproportionation of elemental sulfur. Geochim. Cosmochim. Acta 65 (10), 1601–1609.

Brüchert, V., Pratt, L.M., 1996. Contemporaneous early diagenetic formation of organic and inorganic sulfur in estuarine sediments from St. Andrew Bay, Florida, USA. Geochim. Cosmochim. Acta 60 (13), 2325–2332.

Brüchert, V., Knoblauch, C., Jørgensen, B.B., 2001. Controls on stable sulfur isotope fractionation during bacterial sulfate reduction in Arctic sediments. Geochim. Cosmochim. Acta 65, 763–776.

Calvert, S.E., Thode, H.G., Yeung, D., Karlin, R.E., 1996. A stable isotope study of pyrite formation in the Late Pleistocene and Holocene sediments of the Black Sea. Geochim. Cosmochim. Acta 60, 1261–1270.

Canfield, D.E., 1989. Reactive iron in marine sediments. Geochim. Cosmochim. Acta 53, 619–632.

Canfield, D.E., 2001. Isotope fractionation by natural populations of sulfate-reducing bacteria. Geochim. Cosmochim. Acta 65 (7), 1117–1124.

Canfield, D.E., Thamdrup, B., 1994. The production of ^{34}S-depleted sulfide during bacterial disproportionation of elemental sulfur. Science 266, 1973–1975.

Canfield, D.E., Raiswell, R., Westrich, J.T., Reaves, C.M., Berner, R.A., 1986. The use of chromium reduction in the analysis of reduced inorganic sulfur in sediments and shales. Chem. Geol. 54, 149–155.

Canfield, D.E., Raiswell, R., Bottrell, S., 1992. The reactivity of sedimentary iron minerals toward sulfide. Am. J. Sci. 292, 818–834.

Canfield, D.E., Lyons, T.W., Raiswell, R., 1996. A model for iron deposition to euxinic Black Sea sediments. Am. J. Sci. 296, 818–834.

Canfield, D.E., Boudreau, B.P., Mucci, A., Gundersen, J.K., 1998a. The early diagenetic formation of organic sulfur in the sediments of Mangrove Lake, Bermuda. Geochim. Cosmochim. Acta 62 (5), 767–781.

Canfield, D.E., Thamdrup, B., Fleischer, S., 1998b. Isotope fractionation and sulfur metabolism by pure and enrichment cultures of elemental sulfur-disproportionating bacteria. Limnol. Oceanogr. 43, 253–264.

Canfield, D.E., Habicht, K.S., Thamdrup, B., 2000. The Archean sulfur cycle and the early history of atmospheric oxygen. Science 288, 658–661.

Chambers, L.A., Trudinger, P.A., 1979. Microbiological fractionation of stable sulfur isotopes: a review and critique. Geomicrobiol. J. 1, 249–293.

Chen, C.-T.A., Lin, C.-M., Huang, B.-T., Chang, L.-F., 1996. Stoichiometry of carbon, hydrogen, nitrogen, sulfur and oxygen in the particulate matter of the western North Pacific marginal seas. Mar. Chem. 54, 179–190.

Cline, J.D., 1969. Spectrophotometric determination of hydro-

gen sulfide in natural water. Limnol. Oceanogr. 43, 253–264.

Detmers, J., Brüchert, V., Habicht, K.S., Kuever, J., 2001. Diversity of sulfur isotope fractionations by sulfate-reducing prokaryotes. Appl. Environ. Microbiol. 67, 888–894.

Fry, B., Gest, H., Hayes, J.M., 1985. Isotope effects associated with the anaerobic oxidation of sulfite and thiosulfate by the photosynthetic bacterium, *Chromatium vinosum*. FEMS Microbiol. Lett. 27, 227–232.

Fry, B., Gest, H., Hayes, J.M., 1988. $^{34}S/^{32}S$ fractionation in sulfur cycles catalyzed by anaerobic bacteria. Appl. Environ. Microbiol. 54 (1), 250–256.

Fry, B., Jannasch, H.W., Molyneaux, S.J., Wirsen, C.O., Muramoto, J.A., King, S., 1991. Stable isotope studies of the carbon, nitrogen and sulfur cycles in the Black Sea and the Cariaco Trench. Deep-Sea Res. 38, S1003–S1019.

Garrels, R.M., Lerman, A., 1981. Phanerozoic cycles of sedimentary carbon and sulfur. Proc. Natl. Acad. Sci. 78 (8), 4652–4656.

Garrels, R.M., Lerman, A., 1984. Coupling of the sedimentary sulfur and carbon cycles—an improved model. Am. J. Sci. 284, 989–1007.

Goldhaber, M.B., Kaplan, I.R., 1974. The sulfur cycle. In: Goldberg, E.D. (Ed.), The Sea, vol. 5. Wiley-Interscience, New York, pp. 569–655.

Gransch, J.A., Posthuma, J., 1974. On the origin of sulphur in crudes. In: Tissot, B., Bienner, F. (Eds.), Advances in Organic Geochemistry 1973. Editions Technip, Paris, pp. 727–739.

Habicht, K.S., Canfield, D.E., 1997. Sulfur isotope fractionation during bacterial sulfate reduction in organic-rich sediments. Geochim. Cosmochim. Acta 61, 5351–5361.

Habicht, K.S., Canfield, D.E., 2001. Isotope fractionation by sulfate-reducing natural populations and the isotopic composition of sulfide in marine sediments. Geology 29, 555–558.

Habicht, K.S., Canfield, D.E., Rethmeier, J., 1998. Sulfur isotope fractionation during bacterial reduction and disproportionation of thiosulfate and sulfite. Geochim. Cosmochim. Acta 62 (15), 2585–2595.

Hartgers, W.A., Lopez, J.F., Sinninghe Damsté, J.S., Reiss, C., Maxwell, J.R., Grimalt, J.O., 1997. Sulfur-binding in recent environments: II. Speciation of sulfur andiron and implications for the occurrence of organo-sulfur compounds. Geochim. Cosmochim. Acta 61 (22), 4769–4788.

Hartmann, M., Nielsen, H., 1969. δ^{34}S-Werte in rezenten meeressedimenten und ihre Deutung am Beispiel einiger Sedimentprofile aus der westlichen Ostsee. Geol. Rundsch. 58, 621–655.1.

Holland, H.D., 1973. Systematics of the isotope composition of sulfur in the oceans during the Phanerozoic and its implications for atmospheric oxygen. Geochim. Cosmochim. Acta 37, 2605–2616.

Hughen, K.A., Overpeck, J.T., Peterson, L.C., Anderson, R.F., 1996a. The nature of varved sedimentation in the Cariaco Basin, Venezuela, and its palaeoclimatic significance. In: Kemp, A.E.S. (Ed.), Palaeoclimatology and Palaeoceanography from Laminated Sediments. Geol. Soc., London, pp. 171–183.

Hughen, K.A., Overpeck, J.T., Peterson, L.C., Trumbore, S., 1996b. Rapid climate changes in the tropical Atlantic region during the last deglaciation. Nature 380, 51–54.

Hughen, K.A., Overpeck, J.T., Lehman, S.J., Kashgarian, M., Southon, J., Peterson, L.C., Alley, R., Sigman, D.M., 1998. Deglacial changes in ocean circulation from an extended radiocarbon calibration. Nature 391, 65–68.

Hurtgen, M.T., Lyons, T.W., Ingall, E.D., Cruse, A.M., 1999. Anomalous enrichments of iron monosulfide in euxinic marine sediments and the role of H_2S in iron sulfide transformations: examples from Effingham Inlet, the Orca Basin and the Black Sea. Am. J. Sci. 299, 556–588.

Jørgensen, B.B., 1977. The sulfur cycle of a coastal marine sediment (Limfjorden, Denmark). Limnol. Oceanogr. 22, 814–832.

Jørgensen, B.B., 1990. A thiosulfate shunt in the sulfur cycle of marine sediments. Science 249, 152–154.

Kaplan, I.R., Emery, K.O., Rittenberg, S.C., 1963. The distribution and isotopic abundance of sulphur in recent marine sediments off southern Calfornia. Geochim. Cosmochim. Acta 27, 297–331.

Kohnen, M.E.L., Sinninghe Damsté, J.S., Kock-van Dalen, A.C., ten Haven, H.L., Rullkötter, J., de Leeuw, J.W., 1990. Origin and diagenetic transformations of C_{25} and C_{30} highly branched isoprenoid sulphur compounds: further evidence for the formation of organically bound sulphur during early diagenesis. Geochim. Cosmochim. Acta 54, 3053–3063.

Kohnen, M.E.L., Sinninghe Damsté, J.S., de Leeuw, J.W., 1991a. Biases from natural sulphurization in palaeoenvironmental reconstruction based on hydrocarbon biomarker distributions. Nature 349, 775–778.

Kohnen, M.E.L., Sinninghe Damsté, J.S., ten Haven, H.L., Kock-van Dalen, A.C., Schouten, S., de Leeuw, J.W., 1991b. Identification and geochemical significance of cyclic di- and trisulphides with linear and acyclic isoprenoid skeletons in immature sediments. Geochim. Cosmochim. Acta 55, 3685–3695.

Kok, M.D., Schouten, S., Sinninghe Damsté, J.S., 2000a. Formation of insoluble, nonhydrolyzable, sulfur-rich macromolecules via incorporation of inorganic sulfur species into algal carbohydrates. Geochim. Cosmochim. Acta 64, 2689–2699.

Kok, M.D., Rijpstra, W.I.C., Robertson, L., Volkman, J., Sinninghe Damsté, J.S., 2000b. Early steroid sulfurisation in surface sediments of a permanently stratified lake (Ace Lake, Antarctica). Geochim. Cosmochim. Acta 64, 1425–1436.

Kump, L.R., Garrels, R.M., 1986. Modeling atmospheric O_2 in the global sedimentary redox cycle. Am. J. Sci. 286, 337–360.

Lin, H.L., Peterson, L.C., Overpeck, J.T., Trumbore, S.E., Murray, D.W., 1997. Late Quaternary climate change from δ^{18}O records of multiple species of planktonic foraminifera: high-resolution records from the anoxic Cariaco Basin, Venezuela. Paleoceanography 12, 415–427.

Lyons, T.W., 1997. Sulfur isotope trends and pathways of iron sulfide formation in upper Holocene sediments of the anoxic Black Sea. Geochim. Cosmochim. Acta 61, 3367–3382.

Lyons, T.W., Berner, R.A., 1992. Carbon–sulfur–iron systematics of the uppermost deep-water sediments of the Black Sea. Chem. Geol. 99, 1–27.

Lyons, T.W., Werne, J.P., Hollander, D.J., 2003. Contrasting sulfur geochemistry and Fe/Al and Mo/Al ratios across the last oxic-to-anoxic transition in the Cariaco Basin, Venezuela. Chem. Geol. 195, 131–157 (this volume).

Madrid, V.M., Taylor, G.T., Scranton, M.I., Chistoserdov, A.Y.,

2001. Phylogenetic diversity of bacterial and archaeal communities in the anoxic zone of the Cariaco Basin. Appl. Environ. Microbiol. 67 (4), 1663–1674.

Middelburg, J.J., 1991. Organic carbon, sulphur and iron in recent semi-euxinic sediments of Kau Bay, Indonesia. Geochim. Cosmochim. Acta 55, 815–828.

Mossman, J.R., Aplin, A.C., Curtis, C.D., Coleman, M.L., 1991. Geochemistry of inorganic and organic sulphur in organic-rich sediments from the Peru Margin. Geochim. Cosmochim. Acta 55, 3581–3595.

Newton, R.J., Bottrell, S.H., Dean, S.P., Hatfield, D., Raiswell, R., 1995. An evaluation of the use of the chromous chloride reduction method for isotopic analyses of pyrite in rocks and sediments. Chem. Geol., Isot. Geosci. Sect. 125, 317–320.

Peterson, L.C., Overpeck, J.T., Kipp, N.G., Imbrie, J., 1991. A high-resolution late Quaternary upwelling record from the anoxic Cariaco Basin, Venezuela. Paleoceanography 6, 99–119.

Petsch, S.T., Berner, R.A., 1998. Coupling the geochemical cycles of C, P, Fe, and S: the effects on atmospheric O2 and the isotopic records of carbon and sulfur. Am. J. Sci. 298, 242–246.

Price, F.T., Shieh, Y.N., 1979. Fractionation of sulfur isotopes during laboratory synthesis of pyrite at low temperatures. Chem. Geol. 27, 245–253.

Putschew, A., Scholz-Böttcher, B.M., Rullkötter, J., 1995. Organic geochemistry of sulphur-rich surface sediments of meromictic Lake Cadagno, Swiss Alps. In: Vairavamurthy, M.A., Schoonen, M.A. (Eds.), Geochemical Transformations of Sedimentary Sulfur. ACS Symp. Ser., vol. 612, pp. 59–79.

Putschew, A., Scholz-Böttcher, B.M., Rullkötter, J., 1996. Early diagenesis of organic matter and related sulphur incorporation on surface sediments of meromictic Lake Cadagno in the Swiss Alps. Org. Geochem. 25, 379–390.

Raiswell, R., Berner, R.A., 1985. Pyrite formation in euxinic and semi-euxinic sediments. Am. J. Sci. 285, 710–724.

Raiswell, R., Canfield, D.E., 1996. Rates of reaction between silicate iron and dissolved sulfide in Peru Margin sediments. Geochim. Cosmochim. Acta 60, 2777–2788.

Raiswell, R., Canfield, D.E., 1998. Sources of iron for pyrite formation in marine sediments. Am. J. Sci. 298, 219–245.

Raiswell, R., Buckley, F., Berner, R.A., Anderson, T.F., 1988. Degree of pyritization of iron as a paleoenvironmental indicator of bottom water oxygenation. J. Sediment. Petrol. 58 (5), 812–819.

Raiswell, R., Canfield, D.E., Berner, R.A., 1994. A comparison of iron extraction methods for the determination of degree of pyritisation and the recognition of iron-limited pyrite formation. Chem. Geol. 111, 101–110.

Rees, C.E., Jenkins, W.J., Monster, J., 1978. The sulfur isotopic composition of ocean water sulfate. Geochim. Cosmochim. Acta 42, 377–381.

Richards, F.A., 1975. Cariaco Basin (Trench). Oceanogr. Mar. Biol. Ann. Rev. 13, 11–67.

Rickard, D.T., 1975. Kinetics and mechanism of pyrite formation at low temperatures. Am. J. Sci. 275, 636–652.

Rickard, D., Luhter III, G.W., 1997. Kinetics of pyrite formation by the H_2S oxidation of iron (II) monosulfide in aqueous solutions between 25 and 125 °C: the mechanism. Geochim. Cosmochim. Acta 61, 135–147.

Schoonen, M.A.A., Barnes, H.L., 1991a. Reactions forming pyrite and marcasite from solution: I. Nucleation of FeS_2 below 100 °C. Geochim. Cosmochim. Acta 61, 1495–1504.

Schoonen, M.A.A., Barnes, H.L., 1991b. Reactions forming pyrite and marcasite from solution: II. Via FeS precursors below 100 °C. Geochim. Cosmochim. Acta 61, 1505–1514.

Schouten, S., de Graaf, W., Sinninghe Damsté, J.S., van Driel, G.B., de Leeuw, J.W., 1994. Laboratory simulation of natural sulphurization: II. Reaction of multifunctionalized lipids with inorganic polysulphides at low temperatures. In: Telnæs, N., van Graas, G., Øygard, K. (Eds.), Advances in Organic Geochemistry 1993. Org. Geochem., vol. 22, pp. 825–834.

Shipboard Scientific Party, 1994. Site 1002. In: Sigurdsson, H., Leckie, R.M., Acton, G.D. (Eds.), Proc. Ocean Drill. Program, Initial Rep., vol. 165. College Station, Texas.

Sinninghe Damsté, J.S., de Leeuw, J.W., 1990. Analysis, structure and geochemical significance of organically-bound sulphur in the geosphere: state of the art and future research. In: Durand, B., Behar, F. (Eds.), Advances in Organic Geochemistry 1989. Org. Geochem., vol. 16, pp. 1077–1101.

Sinninghe Damsté, J.S., Rijpstra, W.I.C., de Leeuw, J.W., Schenck, P.A., 1988. Origin of organic sulphur compounds and sulphur-containing high molecular weight substances in sediments and immature crude oils. In: Mattavelli, L., Novelli, L. (Eds.), Advances in Organic Geochemistry 1987. Org. Geochem., vol. 13, pp. 593–606.

Sinninghe Damsté, J.S., Rijpstra, W.I.C., Kock-van Dalen, A.C., de Leeuw, J.W., Schenck, P.A., 1989. Characterization of highly branched isoprenoid thiophenes occurring in sediments and immature crude oils. Org. Geochem. 14, 555–567.

Thamdrup, B., Finster, K., Fossing, H., Hansen, J.W., Jørgensen, B.B., 1994. Thiosulfate and sulfite distributions in pore-water of marine sediments related to manganese, iron, and sulfur geochemistry. Geochim. Cosmochim. Acta 58, 67–73.

Wakeham, S.G., 1990. Algal and bacterial hydrocarbons in particulate matter and interfacial sediment of the Cariaco Trench. Geochim. Cosmochim. Acta 54, 1325–1336.

Wakeham, S.G., Sinninghe Damsté, J.S., Kohnen, M.E.L., de Leeuw, J.W., 1995. Organic sulfur compounds formed during early diagenesis in Black Sea sediments. Geochim. Cosmochim. Acta 59 (3), 521–533.

Werne, J.P., Hollander, D.J., Behrens, A., Schaeffer, P., Albrecht, P., Sinninghe Damsté, J.S.S., 2000a. Timing of early diagenetic sulfurization of organic matter: a precursor–product relationship in Holocene sediments of the anoxic Cariaco Basin, Venezuela. Geochim. Cosmochim. Acta 64, 1741–1881.

Werne, J.P., Hollander, D.J., Lyons, T.W., Peterson, L.C., 2000b. Climate-induced variations in productivity and planktonic ecosystem structure from the Younger Dryas to Holocene in the Cariaco Basin, Venezuela. Paleoceanography 15 (1), 19–29.

Wilkin, R.T., Barnes, H.L., 1996. Pyrite formation by reactions of iron monosulfides with dissolved inorganic and organic sulfur species. Geochim. Cosmochim. Acta 60, 4167–4179.

Wilkin, R.T., Arthur, M.A., Dean, W.E., 1997. History of water-column anoxia in the Black Sea indicated by pyrite framboid size distributions. Earth Planet. Sci. Lett. 148, 517–525.

Wortmann, U.G., Bernasconi, S.M., Böttcher, M.E., 2001. Hypersulfidic deep biosphere indicates extreme sulfur isotope fractionation during single-step microbial sulfate reduction. Geology 29 (7), 647–650.

Zaback, D.A., Pratt, L.M., 1992. Isotope composition and speciation of sulfur in the Miocene Monterey Formation: reevaluation of sulfur reactions during early diagenesis in marine environments. Geochim. Cosmochim. Acta 56, 763–774.

Zaback, D.A., Pratt, L.M., Hayes, J.M., 1993. Transport and reduction of sulfate and immobilization of sulfide in marine black shales. Geology 21, 141–144.

Zopfi, J., Ferdelman, T.G., Jørgensen, B.B., Teske, A., Thamdrup, B., 2001. Influence of water column dynamics on sulfide oxidation and other major biogeochemical processes in the chemocline of Mariager Fjord (Denmark). Mar. Chem. 74, 29–51.